

## Enhancement of TiO<sub>2</sub> nanostructure for super capacitors Application

Rofaida M. Mustaf<sup>1</sup>, Qahtan N. Abdullah<sup>1</sup>, Iftikhar M. Ali<sup>2</sup>

<sup>1,2</sup>Department of Physics, College of Education for Pure Sciences, Tikrit University, Iraq.

<sup>3</sup>Department of Physics, College of Sciences, University of Baghdad, Iraq

---

### ABSTRACT

In this paper, TiO<sub>2</sub> nanoparticles were prepared, in addition to chemically synthesized PANi compounds by oxidation method, added 15% of PANi to 10% of TiO<sub>2</sub> to investigate super capacitance properties of TiO<sub>2</sub> after PANi addition. The structural properties of XRD and FE-SEM for the two materials were studied separately and then for composite. In order to understand the optical properties, UV-Vis spectrometer was used, where the energy gap of titanium oxide was calculated and was 4eV, as well as the polymer material was 4.6eV. The capacity characteristics were also studied and good results were shown for the super capacitors.

**Keywords:** *Enhancement, oxidation, TiO<sub>2</sub> Nanostructure*

### 1. Introduction

Among many metal oxides, titanium oxide has distinct properties such as a wide energy gap, which made it attractive to researchers as it has many applications in various fields in areas of design photodectors [1], gas and biosensors [2], supercapacitors [3], hydrogen production [4] photocatalysts [5] energy storage devices [6], and electro chromic switching [7]. Particularly, one-dimensional TiO<sub>2</sub> nanotube displays invented by anodization of titanium (Ti) have been expansively examined as a auspicious electrode material for super capacitors because of their high surface area, respectable chemical steadiness and wide potential space. In addition, this precipitously focused on TiO<sub>2</sub> nanostructure displays deliver a straight path way for electron transportation laterally the long axis of nanotubes to the Ti foil substrate and can be active right as a supercapacitor electrode. However, the original (without intentional doping or modification) TiO<sub>2</sub> nanostructure displays usually suffer from poor capacitive performance, since TiO<sub>2</sub> is a wide bandgap semiconductor 4.6eV for anatase and 4eV for rutile) [8] with a restricted conductivity. Therefore, large enhancement in conductivity of TiO<sub>2</sub> is desirable for super capacitor electrode materials. It is recognized that intensification

---

\*Corresponding author Rofaida M. Mustaf  
E-mail address:

in electrical conductivity of TiO<sub>2</sub> can be achieved through presenting metal [9] or nonmetal impurities [10] into the oxide, which can produce giver or acceptor conditions in the bandgap and thereby increase the absorption of charge movers. Consequently, numerous exploration efforts relating to the fixing or adjustment of TiO<sub>2</sub> material have been made. For illustration, Nakamura et al. [11] set plasma-treated TiO<sub>2</sub> precipitates by radio-incidence discharge under pressure about 2 Tor of H<sub>2</sub> gas at 673 K. The photocatalytic movement for NO elimination seemed in the observable light area up to 600 nm after giving the TiO<sub>2</sub> powders in the hydrogen plasma. They recognized the better photocatalytic movement of the plasma-treated TiO<sub>2</sub> powders to the anew formed oxygen vacancy situations among the valence and the transmission bands in the TiO<sub>2</sub> band structure. Schmuki et al. [12] indicated that TiO<sub>2</sub> nanotube displays could be rehabilitated to a highly conductive phase by a high-temperature handling in acetylene. The as-prepared C-doped TiO<sub>2</sub> nanotube displays showed semi metallic conductivity, which could be used as a highly effective support for electro catalytic responses. Recently, Lu et al. [13] have revealed that hydrogenation can advance significantly the electrochemical performance of TiO<sub>2</sub> as electrode.

Polymer chains play an important part in the realm of optoelectronics. [14, 15] Between the conjugated polymers, Polyaniline (C<sub>6</sub>H<sub>7</sub>N) has been recognized for extra than a period in its “aniline black” form. Between the showing polymers, polyaniline is the greatest promising polymer due to its low cost, chemical stability [16], manageable electrical conductivity, outstanding ecological stability, Polyaniline has received great attention because it shows controlled susceptibility to electrical conductivity.

## 2. Experimental Work

### 2.1 Synthesis of TiO<sub>2</sub> Nanostructure

In archetypal way for groundwork of TiO<sub>2</sub> nanoparticles, 0.5 g TiO<sub>2</sub> balls were melted in to 30 ml NaOH explanation underneath robust moving at chamber temperature for 2 h. Then the yellowish explanation was treated in an ultrasonic bath (Power Sonic 405, 40 KHz and 350 W) for 2 h in ambient temperature. The resultant precipitates were then centrifuged, wash away and pour out with deionized water numerous times and dehydrated out at 60 °C for 24 h.

### 2.2 Synthesis of PANi

Here are the following steps which have the same procedures of ref. [17]:

- 1- 12.5 mg Solution of Aniline (ANI), monomer was melted in 76 ml of concentrated water with continuous stirring at R.T. for 10 min.
- 2- 0.24 g of Ammonium Persulphate (APS) in 4 ml of purified water was melted with continuous stirring at R.T. for 10 min.
- 3- Solution of **step 2** was added drop wise to resultant solution of **step 1** with continuous stirring.

- 4- the precipitate explanation (black green precipitate) is put on cleaned silicon substrates by using drop cast. (In the dropper, 5 drops were distilled on to glass or silicon until it dried on the heater under a temperature 80 )

### 2.3 Preparation of TiO<sub>2</sub>-PANI nanocomposite

An appropriate amount of PANi was dispersed in distilled water and added to TiO<sub>2</sub> with volume ratios of 10% :15% and subjected to ultrasonic waves for 1 hour to obtain a ready-to-use homogenous dispersion.

### 2.4 Preparation of the electrode

was used for this purpose TiO<sub>2</sub>-PANI and PANi nanocomposite was deposited on it by drop casting method to be ready for supercapacitor examination which is placed in 1.0 ml of sulphuric acid (H<sub>2</sub>SO<sub>4</sub>) and test the curves of the GCD examination, CV measurements in order to calculate its capacity.

Microstructure and structure of the synthesized materials have been characterized using field production skim through electron microscopy (FESEM) and X-ray diffraction (XRD). The visual transmission and absorption spectra of the organic – Polyaniline solutions in the visible and NIR regions (190–1100) nm have been recorded using (UV–Visible 1800 Double beam spectrophotometer). by using drop cast

## 3. Results and Discussion

The structural analysis and development orientation of the prepared nanostructured materials pure TiO<sub>2</sub>, pure PANi, and TiO<sub>2</sub> -PANI were examined by HR-XRD diffraction, the XRD patterns are displayed in Figure (1,2,3). In Figure (1) the exact comparison of the documented XRD patterns with the typical JCPDS card No. TiO<sub>2</sub> Rutile JCPDS card No.-65-5714, and Anatase Tetragonal, JCPDS card No.- 21-1272, confirms the formation of pure TiO<sub>2</sub> phases with two phase Rutile, and Anatase. The peaks appear for the TiO<sub>2</sub>-nanocomposites correspond to different planes of anatase, and rutile TiO<sub>2</sub> respectively. The diffraction patterns of pure TiO<sub>2</sub> were indexed as (110), (101), (111), (200), in addition to the few detected weak peaks indexed as (004), for Rutile and Anatase phase respectively. In figure (2) shows XRD pattern of PANi proves a variety of the diffraction peaks at ranges  $2\theta = 10 - 45$ , because of the amorphous presence of structured by the oxidative polymerization method [18]. The wide peak results from dissipating X-rays from the chain of the PANi [19-20]. Figure (3) illustrates an XRD peaks of the TiO<sub>2</sub>-PANI (%10:15%) nanocomposites. It shows diffraction peaks (101), (111), (210) and (101), (004), planes for Rutile and Anatase phase respectively planes, while the other weak peaks belongs to PANi

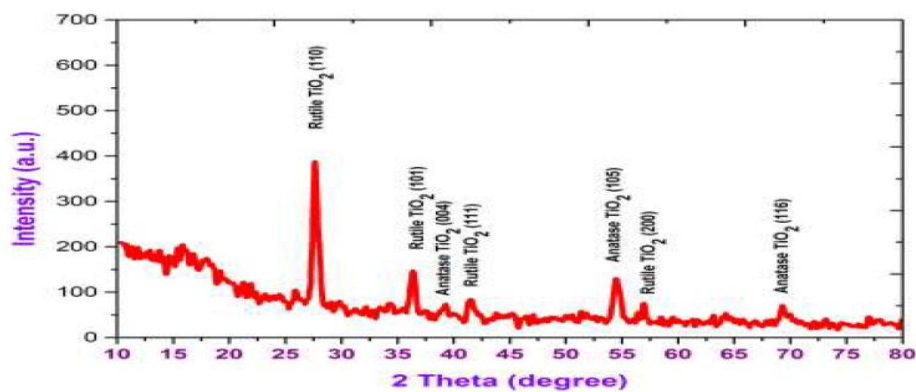


**Figure 1.** Pure  $\text{TiO}_2$

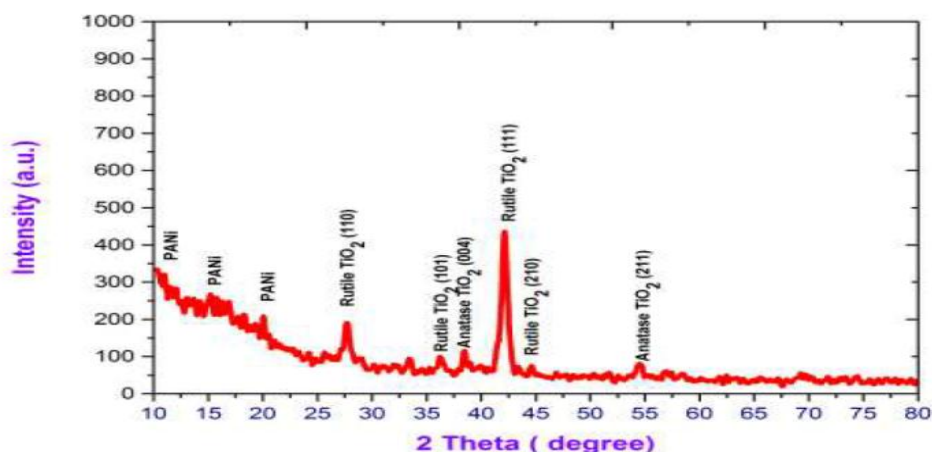


**Figure 2.**  $\text{TiO}_2$  -PANI (10%-15%) nanocomposite grown on Si substrate.

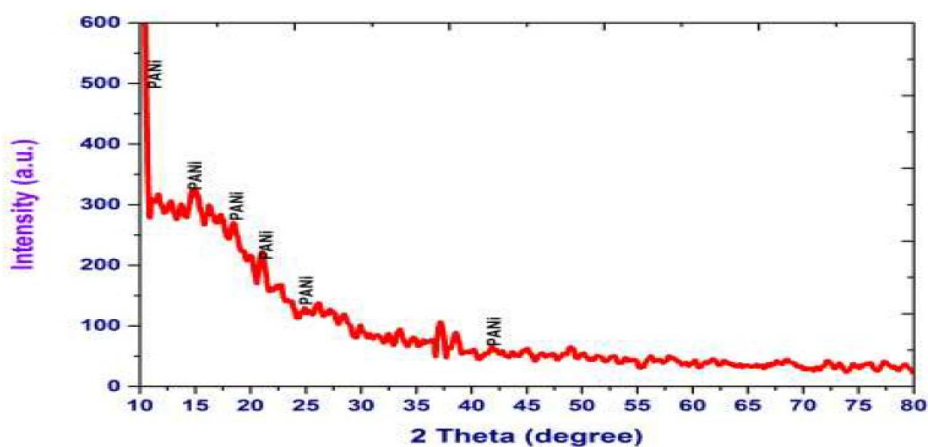


**Figure 3.** pure PANI

Figure(1,2,3) : High resolution X-ray diffraction (HRXRD) patterns of (1) pure  $\text{TiO}_2$  (2)  $\text{TiO}_2$ -PANI (10%:15%) nanocomposite grown on Si substrate (3) pure PANI.

The surface morphology of  $\text{TiO}_2$  and  $\text{TiO}_2$ / PANi composites thin films deposited on a silicon substrate by spin coating technique at room temperature was examined by Field Emission Scanning Electron Microscope (FESEM). FESEM micrographs of nanocrystalline  $\text{TiO}_2$  thin film are shown in (Figure4). From the figure, a randomly distribution of  $\text{TiO}_2$

nanocrystallines over the scanned area can be observed and regular shapes can be clearly noticed. Due to high surface charge, agglomeration takes place according to Ostwald ripening process [21]. The FESEM micrographs of the TiO<sub>2</sub> thin film check that it comprises some pores or voids and vacancies caused by difference in experimental conditions, mainly the semiuniform of solution during deposition, which is in agreement with other reports [21, 22]. The average grain size of TiO<sub>2</sub> nanoparticles was  $45\pm 2$  nm. (The measurements were taken at the University of Tehran)

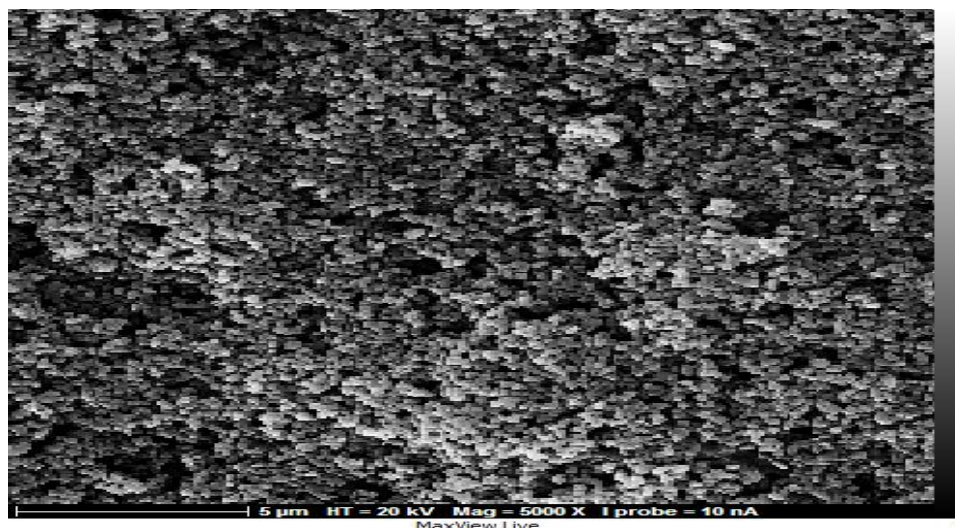


**Figure 4.** FESEM images of pure TiO<sub>2</sub> nanostructures grown on Si substrate

(Figure5) illustrates the images for PANi thin films at low and high magnifications. The FESEM spitting image of Polyaniline obviously point to that the polymer owns nanofiber resembling structure. This image similarly exposes that PANi holds certain apertures or emptiness [23]. The interlocked and entwined structure is also due to stable mixture which allows the easy forking with other fibers developing during polymerization process. This simplifies same nucleation in that way mean fine uniform and interrelated nanofibers of PANi, which is in agreement with other reports [24, 25]. The estimated average fiber diameter of PANi NFs from FESEM was  $30\pm 5$  nm which also verifies the middling crystalline scope.

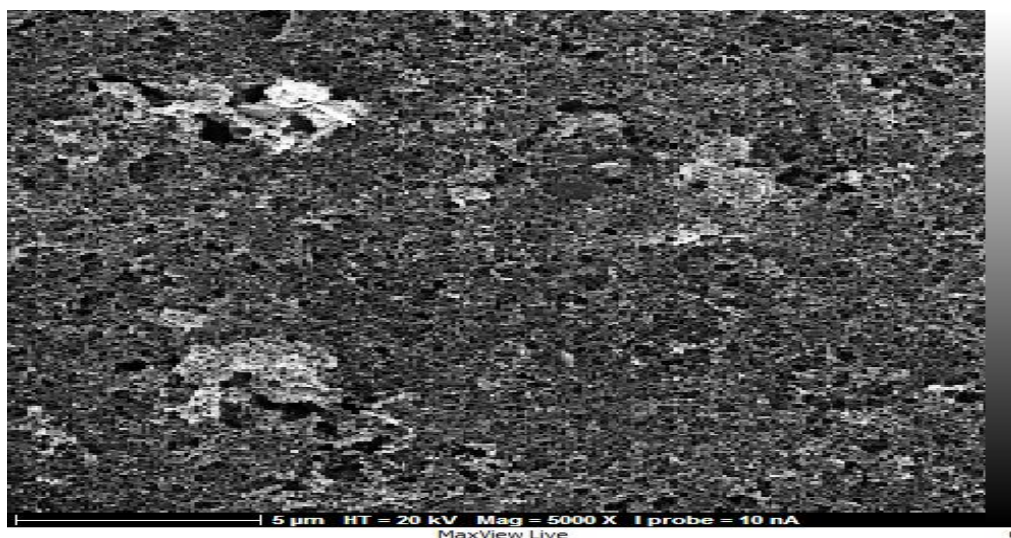


**Figure 5**, FESEM images of pure PANi nanostructures grown on Si substrate

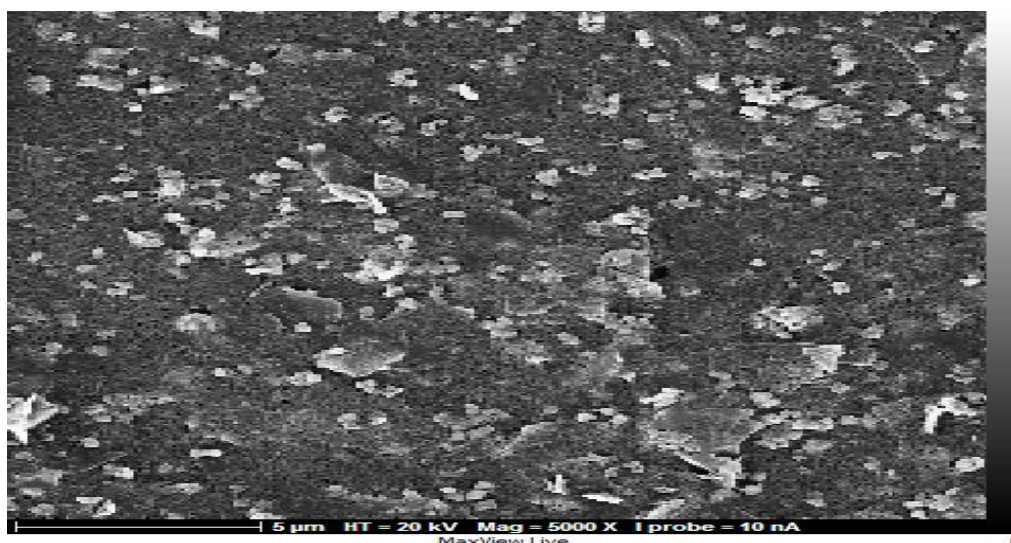


**Figure 6.** shows the resulting mixture of nano fibers for  $\text{TiO}_2$  and nanofibers for PANi in ratio of 10%:15%

For  $\text{TiO}_2$ - PANi thin films which have been deposited on a glass substrate, the values of the optical energy gap ( $E_g$ ) were specified with the use of the Tauc formula as in. It is found that ( $\alpha > 10^4$ ) which means that there is a direct transition of the optical band gap ( $E_g$ ) which is specified through extrapolation of the straight-line helping of the scheme  $(\alpha h\nu)^2$  vs.  $(h\nu)$  for 0 worth of the coefficient of the absorption.  $(\alpha h\nu)^2$  vs.  $(h\nu)$  variation has been depicted in the optical energy gap for  $\text{TiO}_2$  is about 3.3 eV. The obtained band gap is smallest than that of  $\text{TiO}_2$  – PANi that may be ascribed to quantum confinement impacts as a result of the small size of PANi nanostructures, where after adding PANi at different volume ratios (15) volume percent to  $\text{TiO}_2$ , the optical energy gap increased from 4eV to 4.6 eV due to the chemical bonding of  $\text{TiO}_2$  nanoparticles and PANi nano fibers and such variation means that the  $\text{TiO}_2$  nanoparticle electronic characteristics have

been modified strongly by the existence of PANi nanofibers and provide a higher level of the electrical conductivity in composite [26].

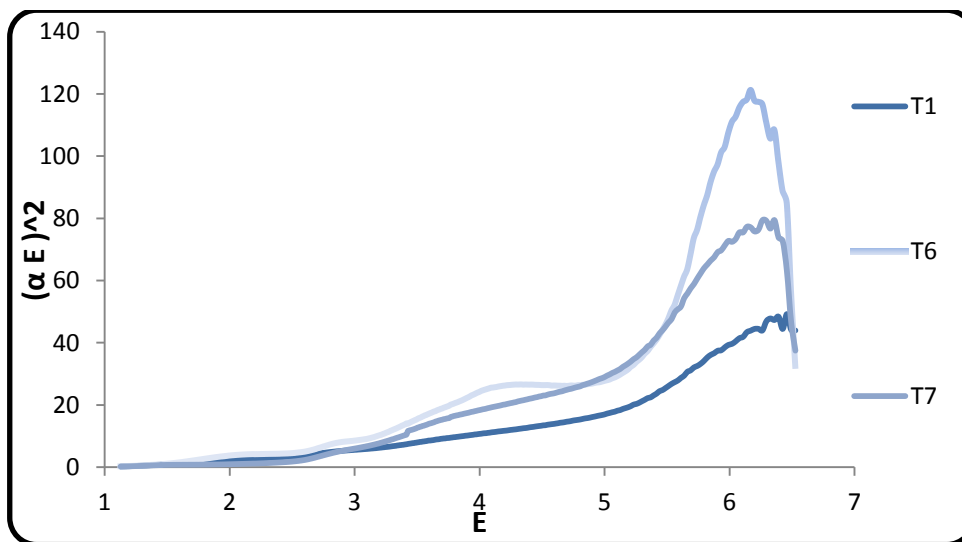


**Figure 7.** Tauc plot of TiO<sub>2</sub> with different volume ratios of PANi.

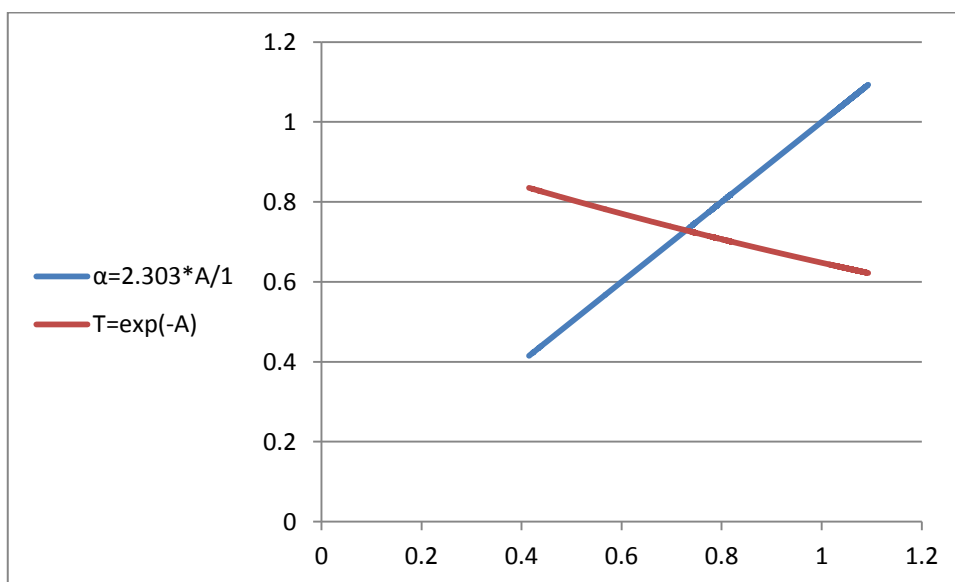


**Figure 8.** TiO<sub>2</sub> pure

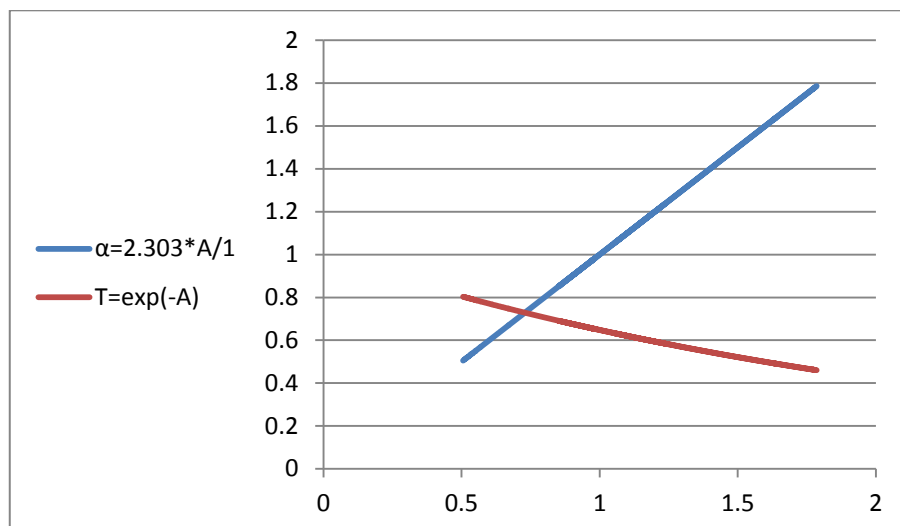


**Figure 9.** TiO<sub>2</sub> – PANi (10%-15%)

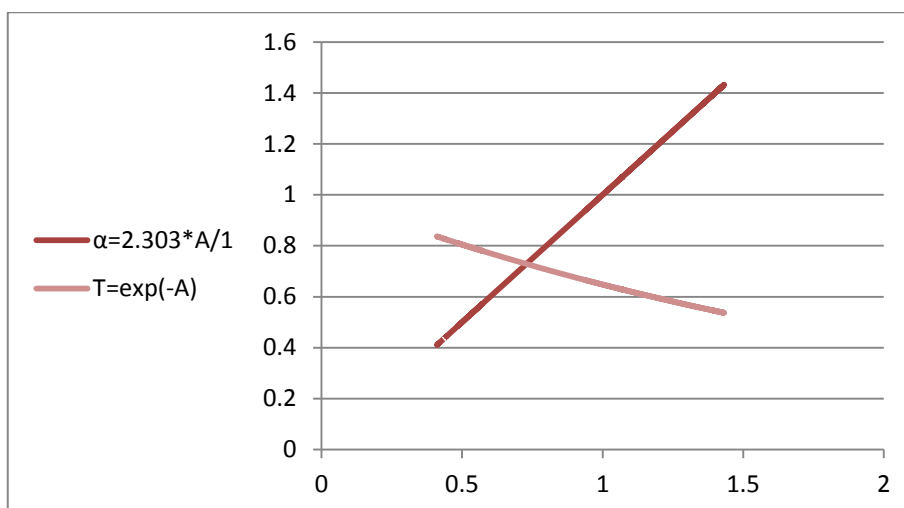


**Figure 10.** PANi pure

For using TiO<sub>2</sub>, PANi and TiO<sub>2</sub>/ PANi as superconductors, cyclic voltammetry (CV) bends were portrayed in Figure 5. by repeating the scan rate, clear peaks of the anode and cathode can be noticed respectively [27]. The results of the Cyclic Voltammetry showed that all of the materials are electro-chemically dynamic in potential territory contemplated. TiO<sub>2</sub> -PANi mixture film incorporates electro-chemical practices of the TiO<sub>2</sub> as well as the PANi. As observed from Figure (6), the nano-organized PANi film terminal experiences an observable electrochemical response underneath a negative potential of - 0.50V. The cathodic procedures may be credited to H<sup>+</sup> addition to the PANi, and anodic procedures compare to H<sup>+</sup> extraction from structure. Such addition procedure can happen in PANi and might be portrayed. During the CVs forms, PANi film is shaded alongside the cathodic procedures and blanched at anodic procedures. Notwithstanding the bend shape, it was seen that the force of the electrochemical



sign is to a great extent expanded in TiO<sub>2</sub>-PAni composites contrasted with TiO<sub>2</sub> or PAni that shows that TiO<sub>2</sub> -Pani materials have higher electro-chemical movement compared to the TiO<sub>2</sub> or PAni. It may be clarified by 2 different means. The first is the synergistic impact of the polyaniline and PAni, and the second is the impact of p-n hetero junctions. PAni acted like an n-type semiconductor, and TiO<sub>2</sub> carried on as a n-type semiconductor. Hence, the p-type TiO<sub>2</sub> formed a p-n intersection with the polyaniline. Consequently, the p-n heterojunctions are liable intended for the way by which the TiO<sub>2</sub>-PAni nanocomposite film had greater charge density compared to the polyaniline film [28].

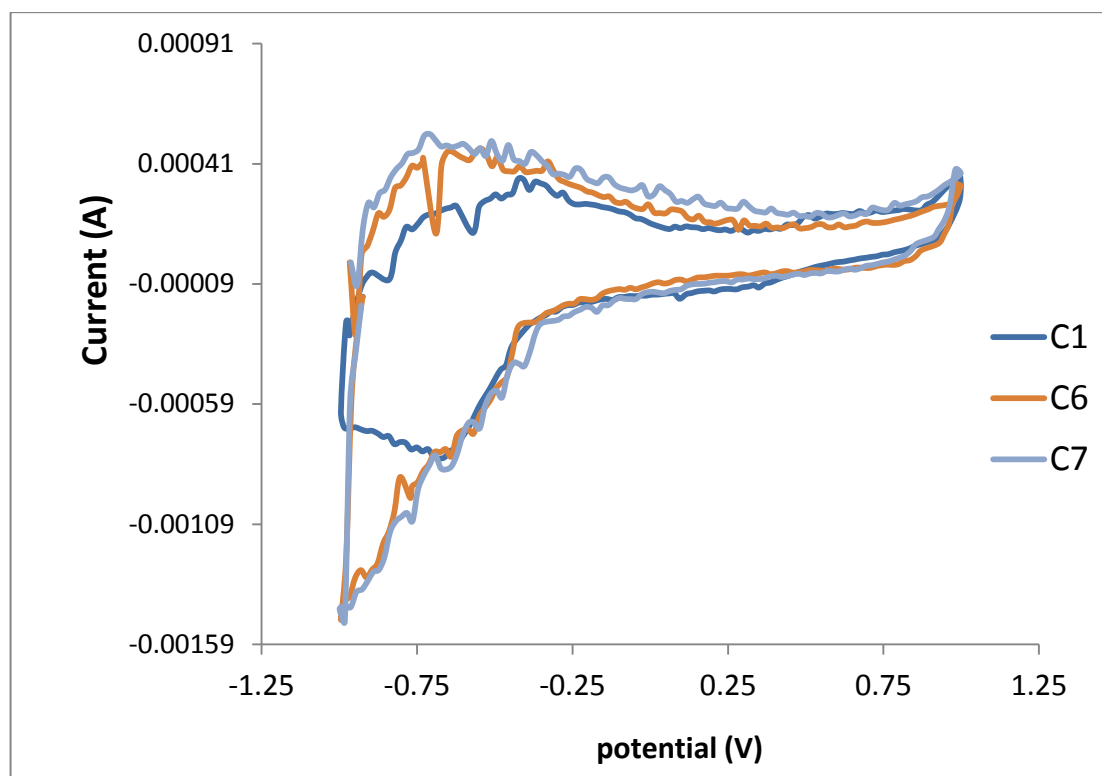


**Figure 11.** Cyclic voltammetry for the pure TiO<sub>2</sub> and TiO<sub>2</sub> -PAni at 50 mV.

#### 4. Conclusions

The TiO<sub>2</sub>-PAni nanocomposites were study successfully by a simple oxidative method. The TiO<sub>2</sub>-PAni nanocomposite has a higher electrochemical movement than that of the pure TiO<sub>2</sub> or PAni. The highest cyclic voltammetry stability of TiO<sub>2</sub>-PAni was at 10% of PAni, The UV-Vis was estimated to calculate the energy gap and was for TiO<sub>2</sub> 4 eV, and the PAni was for 4.6 eV. And it was in a good range.

## 5. References

- [1] O. K. Varghese, M. Paulose, C. A. Grimes (2009). *Long vertically aligned titania nano-tubes on transparent conducting oxide for highly efficient solar cells*, *Nature Nanotechnology* 4(592).
- [2] D. D. Li, P. C. Chang, C. J. Chien, J. G. Lu (2010). Applications of tunable TiO<sub>2</sub> nanotubes as nanotemplate and photovoltaic device, *Chemistry of Materials* 20: 5707
- [3] D. D. Li, C.J. Chien, S. Deora, P.C. Chang, E. Moulin, J.G. Lu (2011). Prototype of scalable core-shell Cu<sub>2</sub>O/TiO<sub>2</sub> solar cell, *Chemical Physics Letters* 501, 446.
- [4] A. Ghicov, S.P. Alba, J. M. Macak, P. Schmuki (2008). *High-contrast electrochromic switching using transparent lift-off layers of self-organized TiO<sub>2</sub> nanotubes*, *Small* 4: 1063.
- [5] H.G. Moon, Y.S. Shim, D. Su, H.H. Park, S.J. Yoon (2011). H.W. Jang, Embossed TiO<sub>2</sub> thin films with tailored links between hollow hemispheres: synthesis and gas-sensing properties, *Journal of Physical Chemistry C*, 115: 9993.
- [6] W. K. Zhang, L. Wang, H. Huang, Y. P. Gan, C.T. Wang, X.Y. Tao (2009), Light energy storage and photoelectrochemical behavior of the titanate nanotube array/Ni(OH)<sub>2</sub> electrode, *Electrochimica Acta*, 54; 4760.
- [7] J.H. Kim, K. Zhu, J.Y. Kim, A.J. Frank (2013), Tailoring oriented TiO<sub>2</sub> nanotube morphology for improved Li storage kinetics, *Electrochimica Acta* 88: 123.
- [8] A. Bendavid, P.J. Martin, A. Jamting, H. Takikawa (1999), Structural and optical properties of titanium oxide thin films deposited by filtered arc deposition, *Thin Solid Films* 355 6-11.
- [9] Z.K. Zheng, B. B. Huang, X. Y. Qin, X. Y. Zhang, Y. Dai, M.H. (2011). Whangbo, Facile in situ synthesis of visible-light plasmonic photocatalysts M@TiO<sub>2</sub> (M=Au, Pt, Ag) and evaluation of their photocatalytic oxidation of benzene to phenol, *Journal of Materials Chemistry*, 21: 9079.
- [10] X. Chen, S. S. Mao (2007). Titanium dioxide nanomaterials: synthesis, properties, modifications, and applications, *Chemical Reviews* 107: 2891.
- [11] I. Nakamura, N. Negishi, S. Kutsuna, T. Ihara, S. Sugihara, E. Takeuchi (2000). Role of oxygen vacancy in the plasma-treated TiO<sub>2</sub> photocatalyst with visible light activity for NO removal, *Journal of Molecular Catalysis A-Chemical* 161: 205.
- [12] R. Hahn, F. Schmidt-Stein, J. Salonen, S. Thiemann, Y.Y. Song, J. Kunze, V.P. Lehto, P. (2009). Schmuki, Semimetallic TiO<sub>2</sub> nanotubes, *Angewandte Chemie-International Edition* 48: 7236.
- [13] X.H. Lu, G.M. Wang, T. Zhai, M.H. Yu, J.Y. Gan, Y.X. Tong, Y. Li (2012). Hydro-generated TiO<sub>2</sub> nanotube arrays for supercapacitors, *Nano Letters* 12: 1690.
- [14] J. Vogelsang, J. and J. M. Lupton (2012). "Solvent vapor annealing of single conjugated polymer chains: Building organic optoelectronic materials from the bottom up, *The journal of physical chemistry letters*, 3(11): 1503-1513.
- [15] C. O. Baker, et al. (2017). Polyaniline nanofibers: broadening applications for conducting polymers, *Chemical Society Reviews*, 46(5): 1510-1525.

- [16] P. Chandrasekhar (2013). *Conducting polymers, fundamentals and applications: a practical approach*, Springer Science & Business Media.
- [17] X. Yang and L. Li (2010). Polypyrrole nanofibers synthesized via reactive template approach and their NH<sub>3</sub> gas sensitivity, *Synth. Met*, 160( 11): 1365–1367.
- [18] S. Srivastava, et al. (2011). Synthesis and characterization of TiO<sub>2</sub> doped polyaniline composites for hydrogen gas sensing. *International Journal of Hydrogen Energy*, 36(10): 6343-6355.
- [19] C. Zhong, C., et al. (2016). *Electrolytes for electrochemical supercapacitors*, CRC press.
- [20] Heng, I., et al. (2019). Low-temperature synthesis of TiO<sub>2</sub> nanocrystals for high performance electrochemical supercapacitors. *Ceramics International*, 45(4): 4990-5000.
- [21] S. M. Sathiya, G. S. Okram and M. A. Jothi (2017). "Structural, optical and electrical properties of copper oxide nanoparticles prepared through microwave assistance, *Advanced Materials Proceedings*, 2(6), 371-377.
- [22] D. M. Jundale, S. T. Navale, G. D. Khuspe, D. S. Dalavi, P. S. Patil and V. B. Patil (2013). Polyaniline–CuO hybrid nanocomposites: synthesis, structural, morphological, optical and electrical transport studies, *J Mater Sci: Mater Electron*, 24(9), 3526–3535.
- [23] CH. Srinivas, D. Srinivasu, B. Kavitha, N. Narsimlu and K. S. Kumar(2012). Synthesis and Characterization of Nano Size Conducting Polyaniline. *IOSR Journal of Applied Physics*, 1(5), pp 12-15,
- [24] A. Abdolahi, E. Hamzah, Z. Ibrahim and S. Hashim (2012). Synthesis of Uniform Polyaniline Nanofibers through Interfacial Polymerization, *Material*, 5(3): 1487-1494.
- [25] A. D. Bhagwat, S. S. Sawant, Ch. M. Mahajan (2016). Facile Rapid Synthesis of Polyaniline (PAni) Nanofibers, *Journal of nano- and electronic physics*, 8(1): 3.
- [26] A. T. Mane, S. T. Navale, R. C. Pawar, C. S. Lee, and V. B. Patil (2015). Microstructural, optical and electrical transport properties of WO<sub>3</sub> nanoparticles coated polypyrrole hybrid nanocomposites, *Synth. Met.*, 199, 187–195, doi: 10.1016/j.synthmet.2014.11.031.
- [27] J. Firas, M. I. Isam M (2021). Preparation of PPy-WO<sub>3</sub> Nano-composite for Supercapacitor Applications. *Iraqi Journal of Science*, 1503-1512.
- [28] C. Dulgerbaki and A. U. Oksuz (2016). Fabricating polypyrrole/tungsten oxide hybrid based electrochromic devices using different ionic liquids, *Polym. Adv. Technol.*, 27(1): 73–81, doi: 10.1002/pat.3601.